



Multi-scale Accommodation Zones Implications to Facies Quality on Synrift Aptian Lacustrine Carbonate Reservoirs from Brazilian Pre-Salt

Pedro Silvany* (Petrobras), Mario Neto (Petrobras), Rodrigo Bunevich (Petrobras), Julio Almeida (UERJ)

Copyright 2023, SBGF - Sociedade Brasileira de Geofísica

This paper was prepared for presentation during the 18th International Congress of the Brazilian Geophysical Society held in Rio de Janeiro, Brazil, 16-19 October 2023.

Contents of this paper were reviewed by the Technical Committee of the 18th International Congress of the Brazilian Geophysical Society and do not necessarily represent any position of the SBGF, its officers or members. Electronic reproduction or storage of any part of this paper for commercial purposes without the written consent of the Brazilian Geophysical Society is prohibited.

Abstract

This paper presents the tectono-sedimentary time and space evolution of a Brazilian Pre-Salt carbonate reservoir. The work was based on interpreting 3D multi-azimuthal high-resolution seismic, wells, and cross-section restoration techniques. The Oil Field is located at the well-known Santos External High (SEH), north of the Tupi oil field—the pioneer accumulation of the largest and most prolific hydrocarbon trend of the 21st century. In the central portion of the SEH, the regional NE-trending faults system that prevails in the Santos Basin bends to NNW and becomes diffused into several low-displacement normal faults. These faults control a series of segmented structural highs, with some holding significant amounts of oil within lower permeability mudstones. The distribution of these rocks is controlled by an NW horst, segmented in three domains by 290° Az and 245° Az relay ramp systems. These structural domains control discontinuous depocenters that evolved during Mid Aptian continuation of rifting (117 Ma). Evolution through time of these domains influenced sedimentary facies' variations, affecting oil's vertical connectivity within the production zones. In this work, we interpret multi-stage fault growth along the NW structural trend as a mechanism for the distribution of reservoir rocks, promoting localized syn-rift footwall uplift of isolated normal faults. Facies quality degradation along syn-rift structural highs impacts the distribution of preferential fluid flow. Therefore, the association of structural elements described in this study demonstrates that shallow water facies were controlled by uplift at the footwall of low displacement normal faults, inducing local lake-level retraction. Such evolution is strongly influenced by displacement transfer along local transfer zones dissecting the structural highs, which in turn controls local structural highs and lows, hence the distribution of high and low-quality reservoir rocks during later phases of rifting.

Introduction

The sedimentary record of rifts and rifted margins is extremely dependent of how catchment areas and structural highs evolve with respect to the main axis of continental extension (Jourdon et al., 2020; Pérez-Gussinyé et al., 2020). The arrangement of topographic elements shaping the internal compartments of sedimentary basins that controls the hydrology of lakes and future marine environments, determines nature of

sedimentary record and, which direct impact in porosity and permeability of reservoir rocks (Martins- Neto & Catuneanu, 2010). In most of rift and rifted margin settings, catchments areas and intervening structural highs are separated by regions of variable distributed deformation (accommodation and transfer zones) (Allken et al., 2012), where a diversity of subsidiary normal and strike-slip faults, and folds interact to accommodate progression of crustal extension (McClay et al. 2002).

The present work aims to understand the tectonic-sedimentary history from the analysis of patterns of seismic reflectors, tied with wells on top of one pre-salt high that composes a transbasinal NW-SE transfer zone (Lourenço et al. 2022, Silvany et al. 2022). The puzzle assembled from point information (3D survey scale) is incomplete and only understood in greater depth if combined with information on the regional scale. Therefore, the following points will be discussed: (i) The geometry and kinematics of this sector of the Santos Basin External High and (ii) Tectonic-sedimentary evolution of the synrift and postrift phases. This integrated workflow allows prediction of vertical depositional heterogeneities and how accommodation zones affect the lateral reservoir continuity and vertical connectivity of production zones, that is the main uncertainty for reservoir characterization and for fluid-flow behavior during hydrocarbon production.

Geological Context

The reservoir rocks correspond to a Meso-Neo Aptian age (117-112 Ma) carbonate platform, seated at the culmination of a series of rotated NE-SW and NW-SE oriented faulted blocks that compose the Santos External High (SEH) (figure 1). At this region the SHE is bounded to the north and south by a transbasinal NW-SE low-relief transfer zone. This condition led to deposition low energy sedimentary facies, dominantly represented by: carbonaceous-siliciclastic mudstone; peloid laminite with crenulate structure; and dolomite-calcite crust laminite. Genesis of these fine-grained sediments is related to physical (sedimentation), bio-induced (microbial) and chemical (crust precipitation) processes. To a lesser extent there are shallow water facies, formed during the decrease of the lake level and footwall uplift, that correspond to incipient microbial shrubs to spherulites (in situ deposits), passing laterally to ooidal to intraclastic grainstones, in a context of relatively high energy formed by action of waves. Also occurs hydrothermal environments with travertine production with anhedral shrubs, being indicative of chemical precipitation. Silica cementation occurs mainly as post-depositional diagenesis.

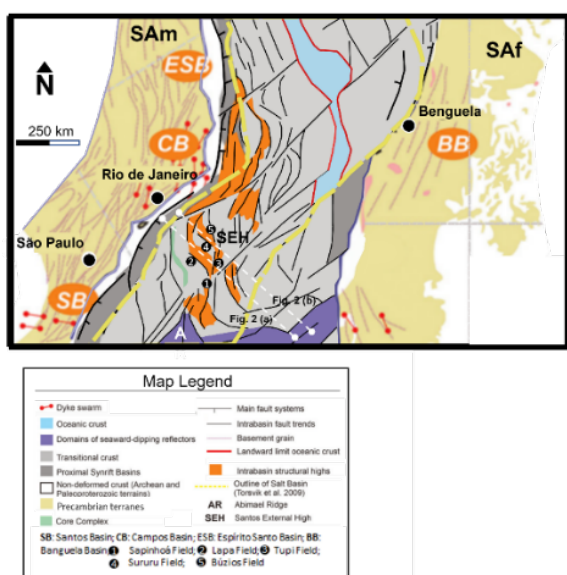


Figure 1 – South America (SAM) and Africa (SAf) shown in a South Atlantic plate reconstruction to 117 Ma. Note the intra-basin architecture, with northern compartments defined by sigmoidal intra-basin fault trends that separate structural lows from structural highs. This region coincides with the area occupied by the Aptian Salt basins of the Central Atlantic. (Modified from Heine et al., 2013, and Araujo et al., 2022).

Data and Methods

For the descriptive analysis of the structural framework, high resolution 3D multi-azimuth seismic data was used. Seismic data was processed with a kirchhoff TTI depth migration operator (PSDM), applied to three non-dedicated conventional narrow azimuth seismic surveys, acquired with sail-lines with 90°, 158° and N122° Az. The regional tectono-sedimentary context was obtained through the interpretation of the ION GXT seismic line 600-1600 (figure 2). This line is part of a survey with 26 seismic lines acquired and processed by ION-GXT (BrasilSpan Project, see Kumar et al. 2013). Six regional unconformities were interpreted, representing the main synrift megasequences of the Santos basin. 256 fault planes and 134 axial planes of seismic-scale folds were described (Figure 3). Structural analysis (pole contour, dip, dip direction) of fault and fold architectures was performed using stereograms and rose diagrams. Families of faults were defined by abutting relationships, being sensitized in synoptical maps. All this validated with section balancing and sequential restoration techniques (Schultz-Ela, 1991, 1992; Rowan, 1993), followed by isostatic adjustment and decompaction (Fetter, 2009). Isostatic adjustment was local, with a fine and discreet mesh, whereas parameters for decompaction of were obtained with adjustment of the power law to a typical sonic porosity profile. For all sections, fault restoration was computed with the move on fault with antithetical shear algorithm.

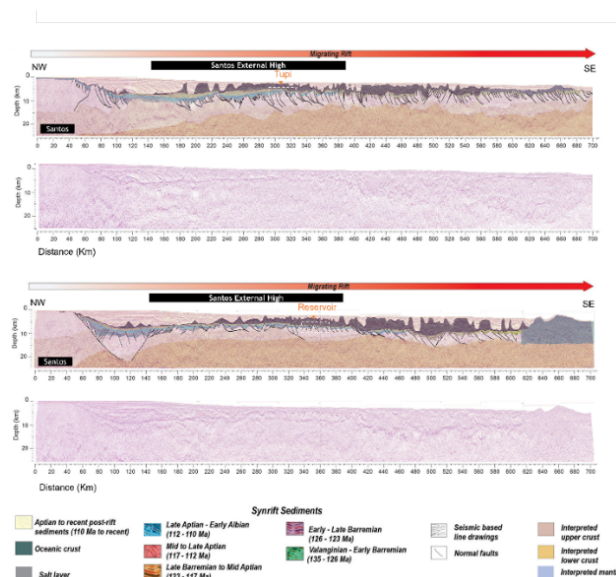


Figure 2 – Interpreted and uninterpreted depth-converted conjugate Santos-Benguela transect through the central portion of the Central Atlantic. For section location, see Figure 1.

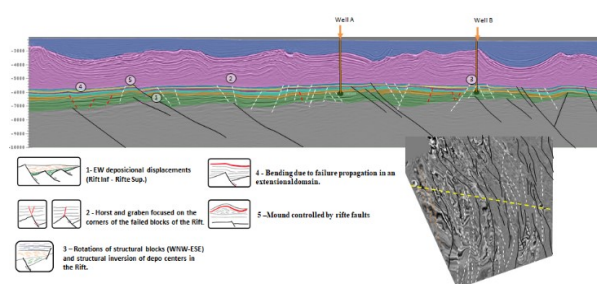


Figure 3 - Seismic section passing through wells A and B, elucidating the main structures of the tectonic-sedimentary framework.

Accommodation Zones and The Impact in the Tectonic sedimentation

The study area displays significant structural variation along their length, such as fault polarity switching that result in generation of segmented subbasins (figures 4). Two oblique narrow accommodation zones separate structural highs (figure 4). These accommodation zones are formed by aligned rely-ramps faults arrays, some of them with opposite dip polarities and divergent tips, which mark depocenters polarity changes (figures 4 and 5). Trend of accommodation zones is subparallel to the WNW-ESE direction of rifting (average value of N290E) in the northern part, and NE-SW in the southern part (average value of N245E) of Santos Basin. Section restoration was applied to predict the major depositional environmental conditions that controlled the spatial facies distribution of an Aptian section platform (Figure 5). Four tectonosedimentary phases were defined: (i) Early syn-rift I (ESRI), (ii) Early syn-rift II

(ESRII), (iii) Late syn-rift (LSR), and (iv) Post-rift (PR). The early formation of half-grabens controlled the initial sedimentation in Early Syn-rift Phase I (ESRI), which generates deposition space filled by siliciclastic rocks (sandstones, conglomerates, shales), and some syngenetic facies composed of talc, stevensite clay, these facies are mainly associated with lacustrine deposits in distal configurations. In Early Syn-rift Phase II (ESRII), amplified half-grabens controlled the sedimentation. Carbonate deposits are mainly represented by coquinas occurrence in the structural highs during the Neobarremian-Eoaptian. The distal parts contain siliciclastic mudstones and dark shales, rich in organic matter. Sandstones and conglomerates occur at the basin's edges, typical of alluvial fans (Figure 6). Decrease in the dip of early syn-rift wedges towards the late syn-rift indicates the progressive interruption of fault activity and the end of the stage in which the mechanical subsidence controls the system's dynamics. The tectonosedimentary maps of the Mid - Late Aptian Early (117 – 113 Ma) deposits show that structural inversions occur during the synrift stage due to the nucleation of antithetic faults, forming horst and grabens geometries (Figures 5, 6). Based on those contrast, we interpret one distinct tectonosedimentary phase, named Late Synrift (LSR). The paleo topographic uplift of the most significant depocenter in the LSR occurs in the Central compartment and is related to the well-8 horst (Figure 5). The localized thinning pattern of the thickness depth maps in the central domain and the depocenters dip direction change for WSW reveal an influence of accommodation zones. Also, the depocenters and structural highs became more discontinuous. This segmentation affects, among other things, lithological contrast such as shallow water facies in an evaporative system which corresponds to incipient microbial shrub to spherulites (in situ deposits), associated with the depositional profile change.

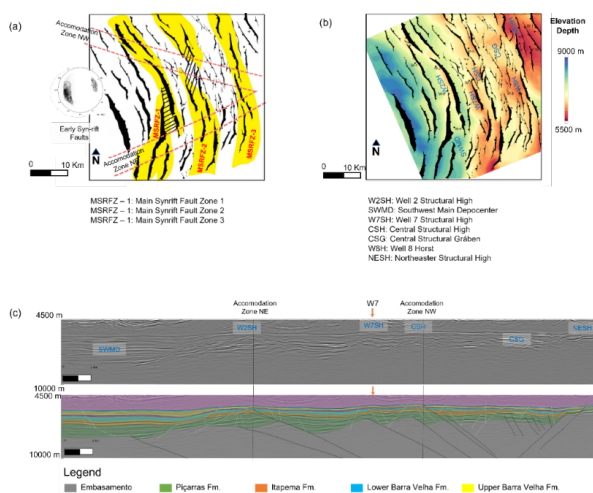


Figure 4 – (a) Structural fault framework of Early syn-rift (ESR) highlighting the geometric characteristics of all Main Syn-rift fault zones (MSRFZ). Notice how the pattern of major faults and structural highs are segmented in the accommodation zone regions. (b) Main early syn-rift fault zones on the structural map of the top of the basement.

(c) Seismic section crossing well 7 elucidating the main structures of the tectonosedimentary framework separated by the accommodation zones.

The development of subaerial travertines is restricted to the central compartment's structural highs near NW's early Synrift faults (Figures 6, 7). The extension travertine is limited by the accommodation zones, which form linear mound occurrence with higher thickness features. Also, mounds near the southwest main depocenters rich in Mg-clay (dehydrated during compaction and lithification) occur near NW early syn-rift faults, which suggests that Mg-clay provided fluids rich in dissolved carbonates possibly influence the occurrence of mounds. The travertine mound occurrence parameters can enhance the prediction of these architectural elements avoiding interpretations pitfalls.

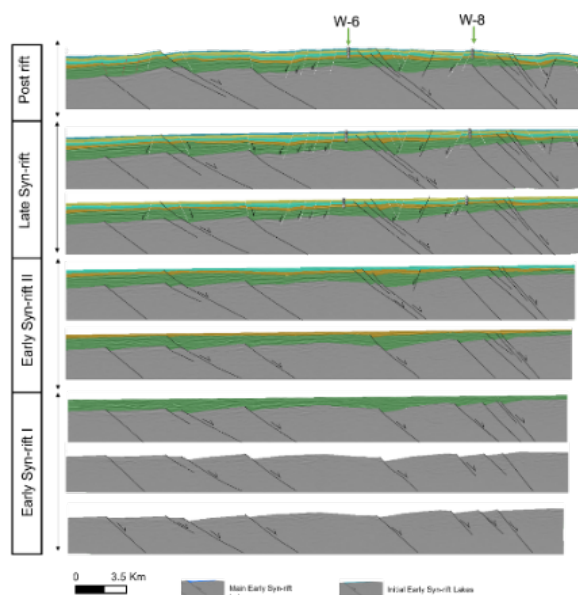


Figure 5 – Restoration steps of section NW-SE crossing wells 6 and 8. Local position of the section is indicated with dashed line in the similarity map.

Conclusions

Footwall uplift generally produces shallow topographic surfaces that control high-energy facies occurrence and drainages that flow away from the structural highs. We observed multi-stage fault growth and interaction in NW structural trend as a mechanism controlling the distribution of reservoir rocks in the oil field during the synrift phase. Such depositional control promotes localized synrift footwall uplift of normal faults with displacement transfer forming systems of accommodation zones. The intervening relief given by diffuse structural highs and lows connected by the accommodation zones controls the distribution of catchment areas for sediments filled with fine-grained rocks and the location of good-quality carbonate rocks at the top of the structural highs. Facies quality degradation along syn-rift structural highs impacts the distribution of preferential fluid flow corridors and reservoir compartmentation. Late Aptian rift-related

faulting controls carbonate platform growth. Shallow water facies occur in relatively high relief horsts, deposited during the relative lake level fall, in an evaporative system which corresponds to incipient microbial shrub to spherulites (in situ deposits), with the gradual lateral transition from ooidal to intraclastic grainstones deposited and reworked by wave action in the relatively high energy context.

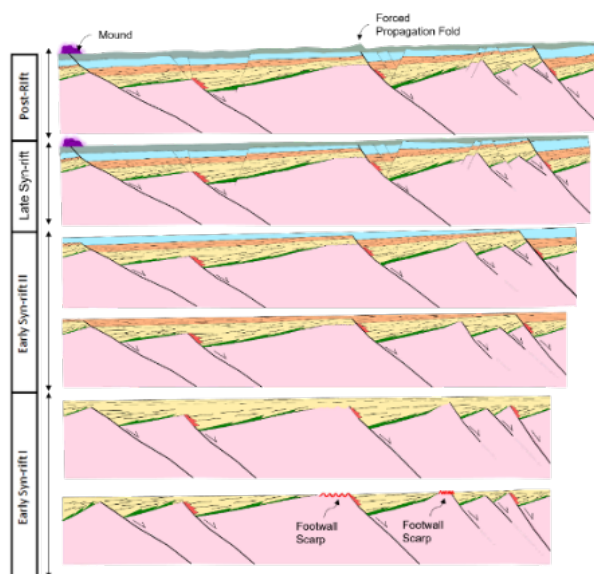


Figure 6 – Schematic representative geological cross-section in the central area for each tectosedimentary phase.

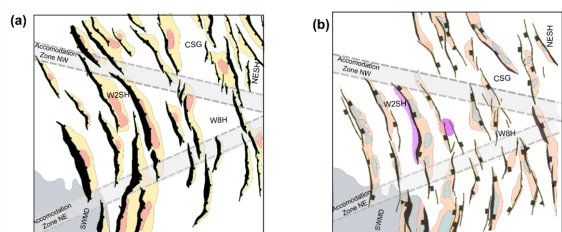


Figure 7 – Schematic model showing the main depocenters of Early syn-rift (top) and Late Syn-rift (bottom) phases. Notice that extension travertine mounds is restricted to the Central Domain and limited by both accommodation zones.

Acknowledgments

We thank Petrobras for permission to publish this work.

References

Allken, V., Huismans, R. S., & Thieulot, C. (2012). Factors controlling the mode of rift interaction in brittle-ductile coupled systems: A 3D numerical study. *Geochemistry, Geophysics, Geosystems*, 13(5), <https://doi.org/10.1029/2012GC004077>.

Araujo, M. N., Pérez-Gussinyé, M., & Muldashev, I. (2022). Oceanward rift migration during formation of Santos–Benguela ultra-wide rifted margins. *Geological Society, London, Special Publications*, 524(1), SP524-2021, <https://doi.org/10.1144/SP524-2021-123>.

Fetter, M. (2009). The role of basement tectonic reactivation on the structural evolution of Campos Basin, offshore Brazil: Evidence from 3D seismic analysis and section restoration. *Marine and Petroleum Geology*, 26(6), 873-886, <https://doi.org/10.1016/j.marpetgeo.2008.06.005>.

Gawthorpe, R. L., & Leeder, M. R. (2000). Tectono-sedimentary evolution of active extensional basins. *Basin Research*, 12(3-4), 195-218, <https://doi.org/10.1111/j.1365-2117.2000.00121.x>.

Heine, C., Zoethout, J., & Müller, R. D. (2013). Kinematics of the South Atlantic rift. *757 Solid Earth*, 4(2), 215-253, <https://doi.org/10.5194/se-4-215-2013>.

Jourdon, A., Mouthereau, F., Le Pourhiet, L., & Callot, J. P. (2020). Topographic and tectonic evolution of mountain belts controlled by salt thickness and rift architecture. *Tectonics*, 39(1), e2019TC005903, <https://doi.org/10.1029/2019TC005903>.

Martins-Neto, M. A., & Catuneanu, O. (2010). Rift sequence stratigraphy. *Marine and Petroleum Geology*, 27(1), 247-253, <https://doi.org/10.1016/j.marpetgeo.2009.08.001>.

McClay, K. R., Dooley, T., Whitehouse, P., & Mills, M. (2002). 4-D evolution of rift systems: Insights from scaled physical models. *AAPG bulletin*, 86(6), 935-959, <https://doi.org/10.1306/61EEDBF2-173E-11D7-8645000102C1865D>.

Kumar, N., Danforth, A., Nuttall, P., Helwig, J., Bird, D. E., & Venkatraman, S. (2013). From oceanic crust to exhumed mantle: A 40 year (1970–2010) perspective on the nature of crust under the Santos Basin, SE Brazil. *Geological Society, London, Special Publications*, 369(1), 147-165, <https://doi.org/10.1144/SP369.16>.

Pérez-Gussinyé, M., Andrés-Martínez, M., Araújo, M., Xin, Y., Armitage, J., & Morgan, J. P. (2020). Lithospheric strength and rift migration controls on synrift stratigraphy and breakup unconformities at rifted margins: Examples from numerical models, the Atlantic and South China Sea Margins. *Tectonics*, 39(12), e2020TC006255, <https://doi.org/10.1029/2020TC006255>.

Rowan, M. G. (1993). A systematic technique for the sequential restoration of salt structures. *Tectonophysics*, 228(3-4), 331-348, [https://doi.org/10.1016/0040-1951\(93\)90347-M](https://doi.org/10.1016/0040-1951(93)90347-M).

Schultz-Ela, D. D. (1991). Practical restoration of extension cross sections. *Geobyte;(United States)*, 6(6).

Silvany Sales, P. H., de Araujo, M. N. C., Brandão Bunevich, R., & de Almeida, J. C. H. Control of Basin-Scale Accommodation Zones on Syn-Rift Aptian Lacustrine Carbonate Reservoirs. Implications for Reservoir Quality Estimates of Brazilian Pre-Salt. *Implications for Reservoir Quality Estimates of Brazilian Pre-Salt*.